Reexamining Gamow-Teller decays near ^{78}Ni

M. F. Alshudifat,[1,2,*] R. Grzywacz,[2,3,4] M. Madurga,[2] C. J. Gross,[3] K. P. Rykaczewski,[3] J. C. Batchelder,[5] C. Bingham,[2,4,6]
I. N. Borzov,[7,8] N. T. Brewer,[9] L. Cartegni,[2] A. Fijałkowska,[2,10] J. H. Hamilton,[9] J. K. Hwang,[9] S. V. Ilyushkin,[11] C. Jost,[2]
M. Karny,[5,10] A. Korgul,[6,10] W. Królas,[6,12] S. H. Liu,[5] C. Mazzocchi,[6,10] A. J. Mendez II,[3] K. Miernik,[3,10] D. Miller,[2]
S. W. Padgett,[2] S. V. Paulauskas,[2] A. V. Ramayya,[9] D. W. Stracener,[3] R. Surman,[13] J. A. Winger,[11]
M. Wolińska-Cichocka,[3,5,14] and E. F. Zganjar[15]

[1]*Department of Physics, Al al-Bayt University, Mafraq 25113, Jordan*
[2]*Department of Physics and Astronomy, University of Tennessee, Knoxville, Tennessee 37996, USA*
[3]*Physics Division, Oak Ridge National Laboratory, Oak Ridge, Tennessee 37830, USA*
[4]*Joint Institute for Nuclear Physics and Applications, Tennessee 37831, USA*
[5]*Oak Ridge Associated Universities, Oak Ridge, Tennessee 37831, USA*
[6]*Joint Institute for Heavy-Ion Research, Oak Ridge, Tennessee 37831, USA*
[7]*National Research Centre "Kurchatov Institute", 123182 Moscow, Russia*
[8]*Joint Institute for Nuclear Research, Dubna 141980, Russia*
[9]*Department of Physics and Astronomy, Vanderbilt University, Nashville, Tennessee 37235, USA*
[10]*Faculty of Physics, University of Warsaw, Warszawa PL 00-681, Poland*
[11]*Department of Physics and Astronomy, Mississippi State University, Mississippi 39762, USA*
[12]*Institute of Nuclear Physics, Polish Academy of Sciences, Kraków PL 31-342, Poland*
[13]*Department of Physics, Union College, Schenectady, New York 12308, USA*
[14]*Heavy Ion Laboratory, University of Warsaw, Warsaw PL 02-093, Poland*
[15]*Department of Physics and Astronomy, Louisiana State University, Baton Rouge, Louisiana 70803, USA*

Decays of neutron-rich nuclei ^{82,83}Zn and ^{82,83}Ga produced in proton-induced fission of ^{238}U were studied at the Holifield Radioactive Ion Beam Facility using on-line mass separation and β-γ spectroscopy techniques. New γ-ray transitions were identified and level schemes, which include states at high excitation energies in the range between 3–7 MeV were constructed. These high-energy levels were identified to be populated through allowed Gamow-Teller β transitions, and their structure was interpreted with new shell-model calculations. A β-delayed neutron branching ratio of $69 \pm 7\%$ was deduced for ^{82}Zn and revised β-decay half-life values of ^{82}Zn [155(17)(20) ms] and ^{83}Zn [122(28) ms] were determined.

I. INTRODUCTION

β-decay properties, including half-lives and branching ratios, are among the most important observables provided by decay spectroscopy experiments. These observables are directly related to the nuclear structure of the parent and daughter nuclei, and thus, the experimental data can be used to inform theory. The sensitivity of the nuclear lifetimes and branching ratios to the presence of the shell closures is among the prime examples. β-decay data on fission products are also needed in nuclear energy applications [1], and for interpretation of antineutrino measurements [2–4] and astrophysical processes [5,6]. In the latter case, the modeling of the r-process nucleosynthesis relies mostly on a global model's ability to predict properties of many nuclei including extrapolation to some nuclei well beyond present experimental reach.

The main purpose of this work is the investigation of β-decay properties of very neutron-rich zinc and gallium isotopes near the doubly magic nucleus ^{78}Ni. The decays of isotopes with $N > 50$ are driven by the competition between the effects of the phase space (energy of β transition) and

nuclear structure (matrix element of a particular β transition). The elementary equation $f t_{1/2} \propto 1/S_\beta$, which connects the nuclear structure to the nuclear lifetimes and decay branching ratios, requires knowledge of the strength distribution S_β and the phase space factor f (Fermi integral). The distribution of S_β depends on parent and daughter nuclear wave functions and selection rules of the β-decay operators. The Gamow-Teller (GT) operator selection rules, where no orbital angular momentum is carried away by the electron and neutrino, allow only transformations of neutrons (protons) into protons (neutrons) occupying spin-orbit partner orbitals [7]. For a sufficiently neutron-rich medium and heavy mass nuclei, the neutrons near the Fermi energy occupy orbitals in a different oscillator shell than the protons, and therefore, GT transitions involve a conversion of deeply bound neutrons. The influence of the phase space factor (f) favors the decays with high decay energy independent of the transition matrix elements. The forbidden transitions [8] are determined by higher-order effects and have at least two orders of magnitude smaller matrix elements than the first-order (allowed) transitions. Typically, the decay properties of neutron-rich nuclei reveal significant β-branching ratios to the levels at low excitation energy. Here, we present the experimental evidence for GT β transitions populating high-energy states in daughter nuclei.
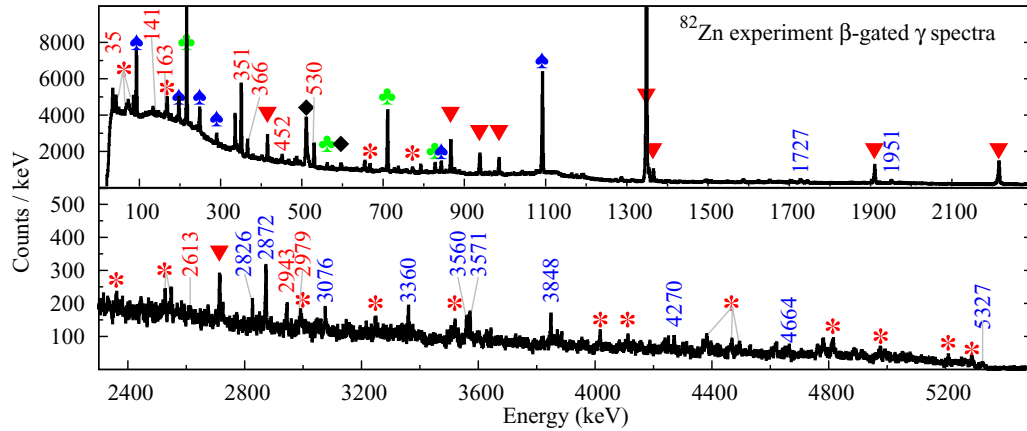
*mohmd7shudif@gmail.com

FIG. 1. ^{82}Zn-decay experiment γ-ray spectrum. The red numbers indicate ^{82}Zn β and βn decay, while the blue numbers indicate new γ-ray transitions in ^{82}Ga β decay. The ▼ represents known γ-ray transitions in ^{82}Ge from ^{82}Ga decay, ♣ and ♠ represents γ-ray transitions in ^{81}Ge and ^{81,82}As, respectively. The ♦ represents annihilation radiation or neutron activation. The ✳ symbol represents unassigned γ-ray transitions.

These experimental data are interpreted within nuclear shell-model calculations.

The β-decay scheme of ^{82}Zn is reported for the first time in this work, while the ^{82}Ga β-decay and partial ^{83}Ga β-decay schemes were previously reported in Refs. [9,10]. New high-energy levels in the respective daughter nuclei were identified and added to the level schemes. These states are interpreted as particle-hole excitations across the $N = 50$ shell gap, which are populated by GT transitions.

The half-lives of ^{82}Zn and ^{83}Zn, 228 ± 10 ms and 117 ± 20 ms, respectively, were determined for the first time using both grow-in and decay curves by Madurga *et al.* [11] using the same data set. A shorter half-life for ^{82}Zn, of 178 ± 3 ms, was reported in the study of relativistic ^{238}U beam fission products [12].

II. EXPERIMENTAL SETUP

The experiments were performed at the Holifield Radioactive Ion Beam Facility (HRIBF) at Oak Ridge National Laboratory. The HRIBF [13] used the isotope separation on-line (ISOL) method for selection of neutron-rich isotopes. A 50 MeV proton beam of $10-18\,\mu$A intensity was used to induce fission in a $6\,\mathrm{g/cm^2}$ thick UCx target. Radioactive

FIG. 2. Decay chains observed in the ^{82}Zn decay experiment.

fission products were transported as vapor and extracted as positive ions at 40 keV. Desired ions of a certain mass ($A = 82$ or 83) were then selected using the first-stage mass separator dipole magnet with mass resolution $m/\Delta m$ of about 1000 located on the high-voltage platform. The ions were accelerated to 200 keV and then transported to the high-resolution second-stage mass separator with mass resolution $m/\Delta m$ of about 10000.

The radioactive ion beam was transmitted to the Low-energy Radioactive Ion Beam Spectroscopy Station (LeRIBSS). Since the gallium isotopes are produced with several orders of magnitude higher rates (in 10^4 and 10^3 pps range at $10\,\mu$A proton beam intensity for ^{82}Ga and ^{84}Ga, respectively, for optimized settings [14]), the use of high-resolution electromagnetic mass separation was used to substantially enhance the relative concentration of zinc, but was not able to completely suppress the Ga contamination in the beam. The evaluation of the data shows about 10% content of ^{82}Zn in the presence of the dominating ^{82}Ga beam component. Similar beam composition was observed in the $A = 83$ measurement with a small percentage of ^{83}Zn ions and the dominating activity of ^{83}Ga.

The radioactive ion beam was implanted into a movable tape at the turnaround point of the moving tape collector (MTC). The implantation spot was located at the center point between four high-purity germanium detectors (HPGe) and two plastic β detectors. The radioactive ion beam was accumulated for four seconds, and then the beam was deflected away for two seconds allowing measurement of the decay of nuclei present in a collected sample. After the decay part of the cycle, the MTC transported the samples approximately 50 cm away from the detectors, behind a 2-in thick lead wall and inside the shielded housing of the MTC. The duration of the tape transport was about 400 ms.

The efficiencies of the HPGe detectors were calibrated with a set of standard radioactive sources in a range from 46 keV up to about 2 MeV. One of the HPGe clovers was excluded from data analysis because of significant amplitude drift. The maximum effective efficiency of the three-clover detection system was 23% at 122 keV and 3.0% at
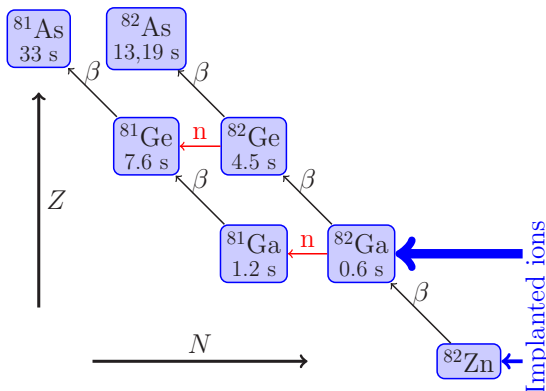
1332 keV. The efficiencies of the HPGe detector at energy values lower than 46 keV can be obtained by extrapolating efficiency points at 46 and 59 keV γ-ray transitions from ^{210}Pb and ^{241}Am, respectively. The plastic scintillator β detectors were used to provide β-trigger signals to reduce the background in the γ spectrum. The efficiencies of the β detectors were calculated by comparing the number of counts in non-β-gated with β-gated singles for energy levels that are only fed by the β decay and deexcite by a single γ-ray transition. The β efficiency was determined to be 39% with a range of ±9%.

The readout of the detection system, including the synchronization pulses of the MTC cycles, was based on the XIA Pixie-16 Rev. D digital electronics modules [15]. All events were recorded by the acquisition system in a triggerless mode and were time stamped with a 100 MHz clock synchronized across all modules. This allowed for setting variable coincidence gates in an off-line analysis.

III. RESULTS AND DISCUSSION

A. β decay of ^{82}Zn and ^{82}Ga

The relevant part of β-gated γ-ray spectrum of the ^{82}Zn β-decay experiment is presented in Fig. 1. It is clearly seen that the ^{82}Ga β decay is dominant in this spectrum, which means that a significant number of ^{82}Ga ions were implanted along with the ^{82}Zn ions.

The γ-γ coincidences with known γ-ray and/or the β-decay half-life were used to make the isotopic assignment for each transition. It was found that the γ-ray spectra corresponding to β decays (β) and β-delayed neutron decays (βn) in chains starting from ^{82}Zn and ^{82}Ga, and ending with ^{81,82}As as shown in Fig. 2. Several γ-ray transitions, such as 85 keV, which is in coincidence with 247, 340, 42, 49, 60, 72, 168 keV transitions seen in the spectrum could not be reliably assigned. Table I lists the energy levels in ^{82}Ga and ^{82}Ge with the associated γ decays and its relative intensity (I_γ) for each decay.

Most of the γ-ray transitions associated with ^{82}Zn β decay are presented here for the first time along with the transitions establishing new high-energy levels in ^{82}Ge. The isomeric γ-ray transition (141 keV) was observed by Kameda *et al.* [16].

1. Decay scheme of ^{82}Ga

The decay of $N = 51$ ^{82}Ga was studied previously by Hoff and Fogelberg *et al.* [17]. The β-delayed neutron branching ratio (P_n) was measured to be 19.8(10)% by Warner and Reeder [18]. An important observable needed for the construction of the level scheme is the feeding to the ground state of the daughter nucleus (^{82}Ge), and it can be inferred from the comparative half-life log(ft) systematics. The ground-state spin of ^{82}Ga was studied using laser spectroscopy [19] and it was found to be $J^\pi = 2^-$. The β transition from ^{82}Ga to ^{82}Ge ground state (0^+) is of the first-forbidden unique type with average log(ft) value of 9.5 ± 0.8 and small direct feeding would result in $I_\beta \leqslant 1\%$ [20], using $Q_\beta = 12.484(3)$ MeV [21]. Based on previously reported data and new information from γ-γ coincidence spectra (Fig. 3) and the revised γ-ray intensities we were able to construct a

TABLE I. Energy levels (E_{levels}) in ^{82,81}Ga and ^{82,81}Ge from β decay of ^{82,81}Zn and ^{82,81}Ga, respectively.

E_{level} (keV)	E_γ	I_γ	Final level (keV)
^{82}Zn β decay			
34.5(1)	34.5(1)	24.2(25)	0
140.7(3)	140.7(3)[a]	1.7(7)	0
366.3(2)	366.3(2)	22.7(30)	0
530.0(5)	163.3(2)	3.5(4)	366.3(2)
	530.0(5)	10.0(10)	0
2978.7(6)	2612.9(11)	11.5(50)	366.3(2)
	2943.8(4)	23.7(49)	34.5(1)
	2978.7(6)	2.4(19)	0
^{82}Zn βn decay			
350.8(1)	350.8(1)	100.0(5)	0
802.3(4)	451.5(3)	13.0(49)	350.8(1)
^{82}Ga β decay			
1348.3(1)	1348.3(1)	100(7)	0
1951.5(2)	1951.5(2)[b]	1.8(4)	0
2215.9(2)	867.0(1)	10.3(14)	1348.3(1)
	2215.9(2)	18.5(37)	0
2286.6(1)	938.3(1)	7.2(1)	1348.3(1)
2333.6(1)	985.3(1)	4.7(6)	1348.3(1)
2702(1)	415.4(1)	2.6(1)	2286.6(1)
	1354(1)	6.5(12)	1348.3(1)
2714.3(9)	1365.4(2)	3.5(6)	1348.3(1)
	2714.3(9)	3.2(5)	0
2826.6(3)	2826.6(3)[b]	0.8(2)	0
3076.3(6)	1727.4(2)[b]	1.5(4)	1348.3(1)
	3076.3(6)[b]	1.3(3)	0
3258(1)	1910.2(2)	10.9(12)	1348.3(1)
3571.4(5)	3571.4(5)[b]	1.8(4)	0
3848.4(3)	3848.4(3)[b]	2.3(4)	0
4221(1)	2872.6(2)[b]	3.3(5)	1348.3(1)
5618(1)	4269.9(2)[b]	1.4(3)	1348.3(1)
6012(1)	4664.1(4)[b]	0.9(2)	1348.3(1)
6063(1)	3360.6(3)[b]	1.8(4)	2702(1)
6675(1)	5326.7(2)[b]	0.10(4)	1348.3(1)
6819(1)	3560.1(5)[b]	1.8(4)	3258(1)
^{82}Ga βn-decay			
679(11)			0
711.1(5)	711.1(5)	12.4(14)	0
895.4(3)	216.4(4)	8.2(9)	679(11)
1241.3(7)	530.0(5)	0.6(1)	711.1(5)
	562.4(5)[c]	0.6(2)	679(11)
1287.7(8)	1287.7(8)[c]	1.8(4)	0
1723.5(5)	482.6(3)[c]	0.4(1)	1241.3(7)
	828.1(5)[c]	2.1(3)	895.4(3)
1730.4(8)	1019.3(6)[c]	0.8(3)	711.1(5)
1831.8(6)	936.4(5)[c]	0.7(2	895.4(3)
2548.3(7)	2548.3(7)[c]	1.5(4)	0
2996.0(10)	1272.5(11)[c]	0.6(2)	1723.5(5)
3436.5(7)	1713.4(5)[c]	0.3(1)	1723.5(5)
	2725.0(10)[c]	0.7(2)	711.1(5)

[a]Isomeric γ transition.
[b]Observed for the first time.
[c]Observed in ^{82}Ga βn-decay channel for the first time.
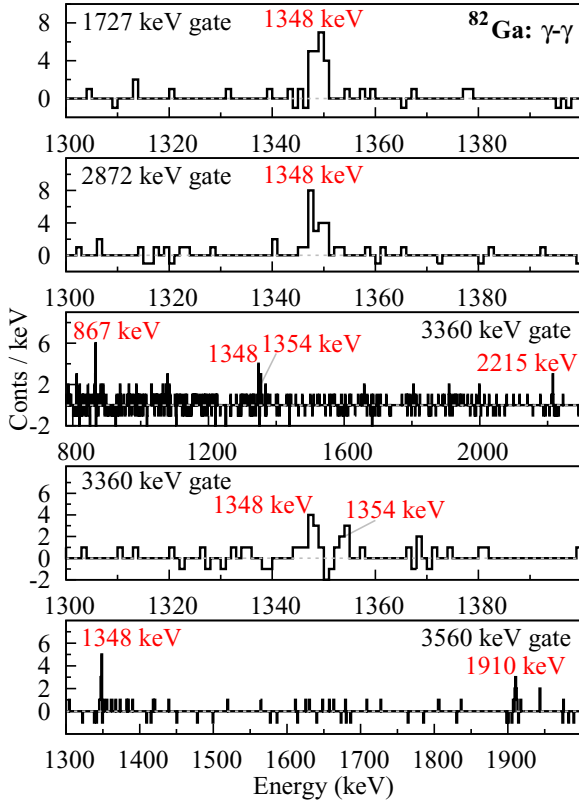
FIG. 3. Part of γ-γ coincidence spectra of relevant γ-ray transitions in the β decay of ^{82}Ga.

^{82}Ga β-decay scheme as presented in Fig. 4. When compared with the previously reported data, we have added several levels to this decay scheme at 3076, 3258, 4221, 5618, 6012, 6063, 6675, and 6819 keV, and tentatively at 1952, 2827, 3571, and 3848 keV. The apparent branching ratios and log(ft) values for assigned transitions fluctuating around 6.0 are similar to high-energy transitions observed in decays of other $N > 50$ nuclei, e.g., ^{81}Zn [22], ^{83}Ge [23], or ^{89,90}Br [24].

Previously assigned spins to 2216, 2286, and 2334 keV energy levels were included in the ^{82}Ga decay scheme (Fig. 4) [26]. The inconsistency between the log(ft) values and the assigned spin for these levels may be due to some amount of missing feeding to these levels. More than 10 observed γ-ray transitions at energies greater than 3 MeV were neither assigned nor placed in the level scheme because of insufficient statistics.

The previously reported [27] γ-ray transitions of 216, 530, and 711 keV in ^{81}Ge were observed in the βn-decay channel of ^{82}Ga. Also using information on the levels assigned to β decay of ^{81}Ga [27], we were able to identify several states in ^{81}Ge, which are populated in the βn channel, see Fig. 5. The levels are observed up to 3.5 MeV excitation energy in ^{81}Ge, and that means that the excited states up to about 10 MeV in ^{82}Ge are populated in β decay.

2. Decay scheme of ^{82}*Zn*

^{82}Zn decays via β and βn channels. The β channel decay scheme was constructed using similar assumptions as in the

^{82}Ga case. The ground-state spin of even-even ^{82}Zn is 0^+, and the ground state of ^{82}Ga (2^-). The ground state to ground state would be a first-forbidden unique transition, and thus, would have a very small branching ratio ($\leqslant 1\%$) with $Q_\beta = 10.3(3)$ MeV [21].

The absolute normalization of γ intensities in the βn channel of ^{82}Zn decay was based on the knowledge of the details of β decay of ^{81}Ga. The 828 keV γ ray can be observed through the ^{81}Ga β-decay channel only; it has 22.1% absolute branching ratio [27]. The number of γ-ray counts that are produced by βn decay of ^{82}Zn should be equal to the total number of counts produced by ^{81}Ga β decay since ^{82}Zn βn decay is the only source for ^{81}Ga in this analysis. The total number of ^{81}Ga β decays can be calculated as follows:

$$N_T^\beta(^{81}\mathrm{Ga}) = \frac{N(828\ \mathrm{keV})}{\mathrm{BR}_\gamma(828\ \mathrm{keV})},$$

where $BR_\gamma(828\ \mathrm{keV}) = 21.7(1)\%$ is the 828 keV γ-ray absolute branching ratio [27] and $N(828\ \mathrm{keV})$ is the total number of counts of 828 keV γ-ray transition calculated from the experimental data. Since the cycle beam-on and beam-off durations were four and two seconds, respectively, and ^{82}Zn has a short β-decay half-life, it will decay out completely. However, the β-decay half-life of ^{81}Ga is 1.2 seconds and, therefore, a certain fraction of ^{81}Ga ions will not have time to decay before they are removed from the detection point. Since the only source for ^{81}Ga is the βn decay of ^{82}Zn, the number (N_1) of created ^{81}Ga atoms is related to βn-decay rate (I_0) of ^{82}Zn by the following relation,

$$N_1(t) = \int I_0(t)dt.$$

The βn-decay rate of ^{82}Zn can be expressed regarding "grow-in" and "decay" parts of the cycle:

$$I_0(t) = \begin{cases} A_0(1 - e^{-t/\tau_0}) & 0 < t < t_1, \\ A_0(e^{t_1/\tau_0} - 1)e^{-t/\tau_0} & t_1 < t < t_2, \end{cases} \quad (1)$$

where $t_1 = 4$, $t_2 = 6$ seconds, $0 < t < t_1$ seconds represent the grow-in interval, $t_1 < t < t_2$ seconds represent the decay interval, $\tau_0 = T_{1/2}(^{82}\mathrm{Zn})/\ln(2) = 0.224$ second, A_0 is the ^{82}Zn implantation rate times the βn branching ratio. The total amount of ^{81}Ga generated in the ^{82}Zn decay is

$$
\begin{aligned}
N_1 = A_0 \bigg(&\int_0^{t_1} (1 - e^{-t/\tau_0})dt \\
&+ \int_{t_1}^{t_2} (e^{t_1/\tau_0} - 1)e^{-t/\tau_0}dt \bigg) \\
&= 4.00 \times A_0.
\end{aligned}
\quad (2)
$$

The number of ^{81}Ga that will not decay within the six seconds duration of the measurement cycle (N_{1R}) can be calculated using the basic decay equation

$$N_{1R} = \int_0^{t_2} e^{-\frac{t_2 - t}{\tau'}} I_0(t)dt,$$

where $\tau' = 1.756(7)$ seconds is the β-decay lifetime of ^{81}Ga [27]. By using βn-decay rate of ^{82}Zn Eq. (1) in the
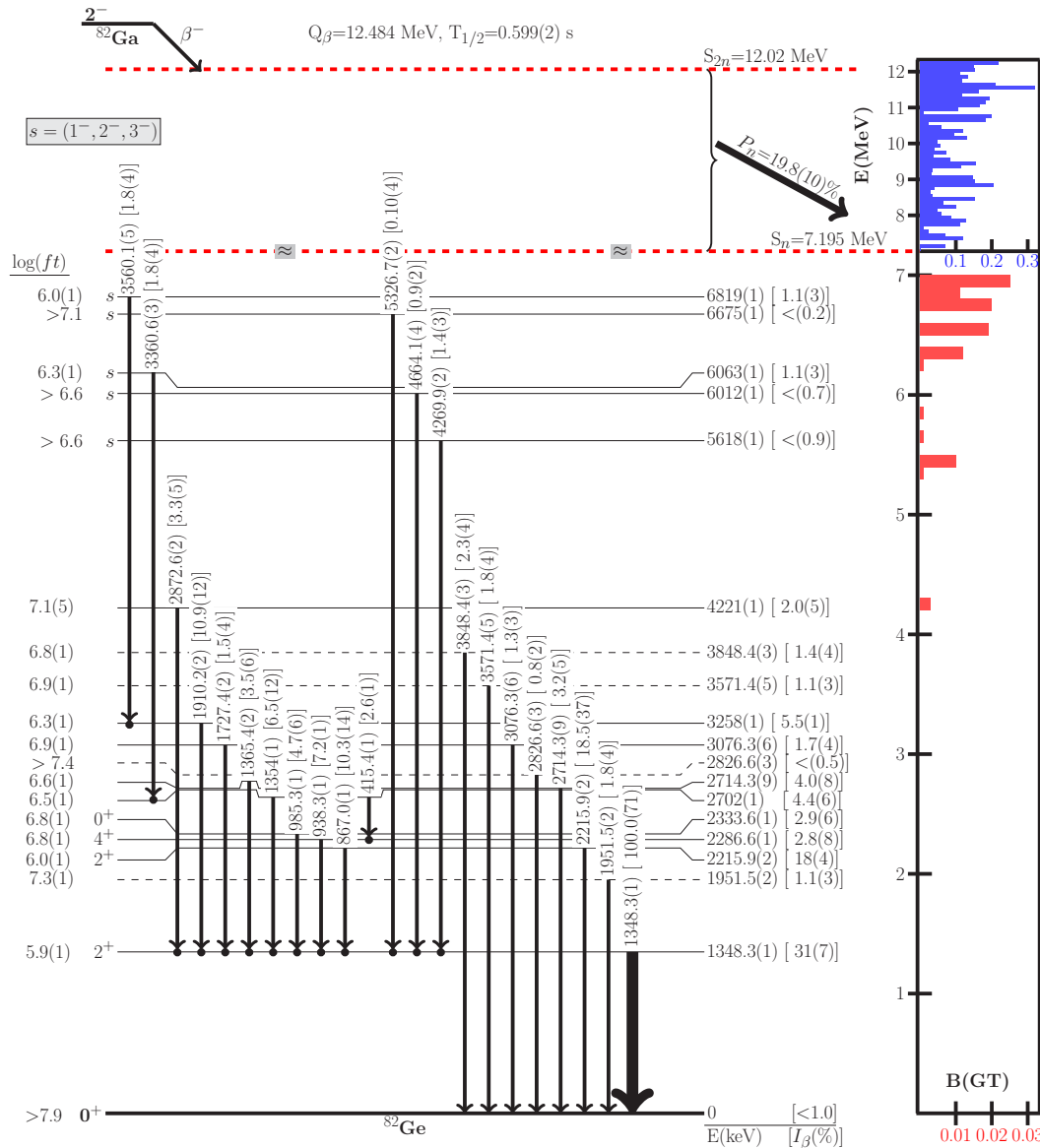
FIG. 4. Decay scheme of ^{82}Ga including all the observed γ-ray transition energies in keV followed by the intensities relative to strongest observed transition given in square brackets along with a theoretically calculated B(GT) distribution (see Sec. IV) vs the excitation energy. Note that the spin assignments for the high-energy states are uncertain, and we propose $s = (1^-, 2^-, 3^-)$ in accordance with the GT selection rules, and the B(GT) histogram in the region below the S_n has a different scale than the histogram above S_n. Due to the possibility that many transitions may have been unobserved or could not be assigned, the absolute feedings are calculated to be consistent with the observed intensities, but may not necessarily reflect the reality. The neutron separation energy and emission probability were taken from Ref. [25].

last integral we get

$$N_{1R} = A_0 \left(\int_0^{t_1} (1 - e^{-t/\tau_0}) e^{-\frac{t_2-t}{\tau'}} dt \right.$$
$$\left. + \int_{t_1}^{t_2} (e^{t_1/\tau_0} - 1) e^{-t/\tau_0} e^{-\frac{t_2-t}{\tau'}} dt \right)$$
$$= 0.56 \times A_0. \qquad (3)$$

The fraction of ^{81}Ga that have not decayed is 14% and was found by comparing Eqs. (2) and (3). Therefore, the total 828 keV γ-ray measured counts must be corrected by a factor of 4.00/3.44 to give the correct number of counts produced by

the βn-decay channel of ^{82}Zn, which becomes

$$N_T^{\beta n}(^{82}\text{Zn}) = 4.00/3.44 \times N_T^\beta(^{81}\text{Ga}). \qquad (4)$$

This value ($N_T^{\beta n}$) represents the total feeding for both the excited states and ground state in ^{81}Ga. The only transition observed that directly feeds the ground state in this analysis is at 351 keV. By subtracting the counts of this transition from the total number of counts in the βn-decay channel of ^{82}Zn, we get the counts that directly feed the ground state.
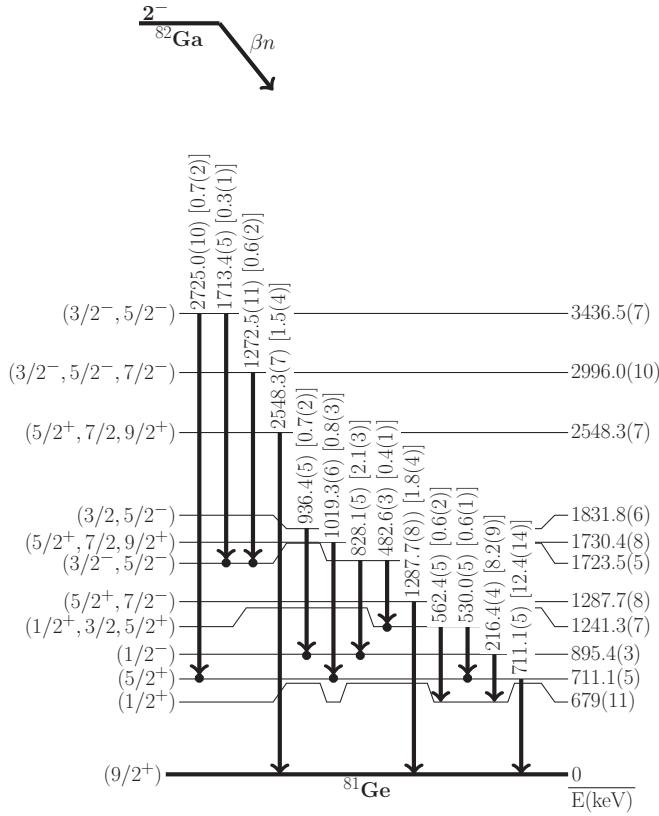
FIG. 5. Energy level scheme deduced for ^{82}Ga βn decay including all the observed γ-ray transition energies in keV followed by the intensities relative to 1348 keV transition observed in ^{82}Ga β decay given in square brackets.

FIG. 6. Selected background subtracted γ-γ coincidences of relevant γ rays in ^{82}Zn β decay.

The ^{82}Zn β-delayed neutron branching ratio was calculated using both Eqs. (5) and (6)

$$P_n = \frac{1}{1+R},\qquad(5)$$

where R represent the ratio between the total counts in the β-decay channel to the total counts in the βn-decay channel of ^{82}Zn as shown in Eq. (6)

$$R = \frac{N_T^{\beta}(^{82}\text{Zn})}{N_T^{\beta n}(^{82}\text{Zn})},\qquad(6)$$

which is equal to 0.45 ± 0.14. The calculated neutron branching ratio was found to be $69 \pm 7\%$.

The decay scheme of ^{82}Zn was based on the experimentally calculated intensities and the γ-γ coincidence spectra (see Fig. 6). Figure 7 represents the β and βn decay of ^{82}Zn. We have identified and assigned several levels previously unknown in ^{82}Ga, which were populated either directly or in the decay of high-energy states. Similar to the decay of other $N > 50$ isotopes, we searched for evidence of high-energy levels, which would provide evidence for GT decay. A strongly populated level at 2979 keV was identified and assigned through the γ-γ coincidence analysis to ^{82}Ga. Based on the $\log(ft) = 4.8$, this level appears to be populated by a GT transition. Thus, we assign spin and parity of $I^{\pi} = 1^+$.
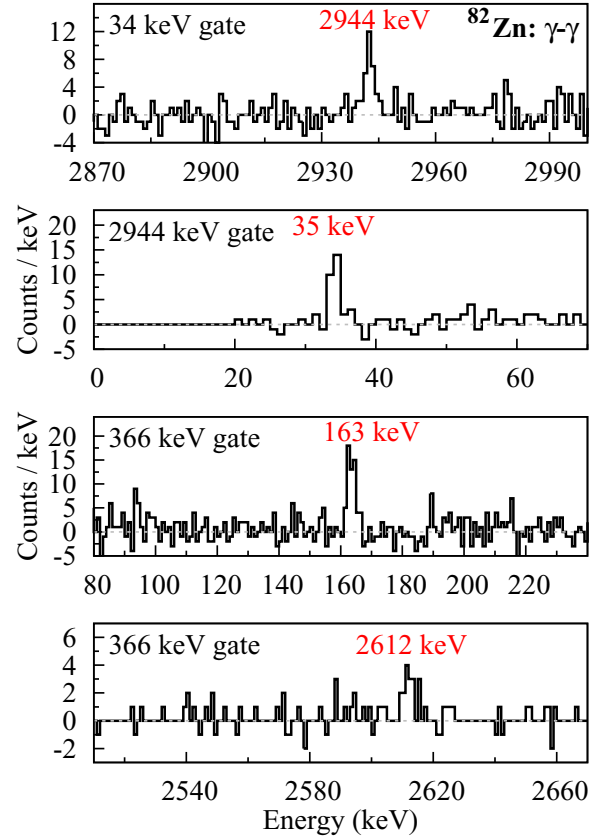
The tentative spin assignments of other low-energy levels populated in the ^{82}Zn decay are based on the assumption that they are either populated directly in first-forbidden transitions (530 and 366 keV) or from the decay of the 1^+ state. The 141 and 34.5 keV states have very small if any, direct population in the β decay. Therefore, we can conclude that their spins have to be $J = 2$ or larger. The 34.5 keV level does not appear to have a measurable lifetime (<10 ns), so we inferred from this that it is deexcited via M1 transition, and therefore, its spin and parity is likely to be 2^- or 3^-. The deexcitation of the isomeric 141 keV level is consistent with E2 γ-ray transition due to its observed half-life of 89 ± 9 ns compare to 98 ± 10 ns from Kameda *et al.* [16] and the likely spin and parity of this state is 4^-.

A comparison between the total intensity of ^{82}Zn and ^{82}Ga decays was used to calculate the fraction of ^{82}Zn ions $F(^{82}\text{Zn})$ presented in the radioactive ion beam (RIB) of this experiment and found to be

$$F(^{82}\text{Zn}) = \frac{N_T(^{82}\text{Zn})}{\frac{N_T^{\beta}(^{82}\text{Ga})}{\text{BR}_{\beta}(^{82}\text{Ga})} - N_T^{\beta}(^{82}\text{Zn})},$$

where N_T represent the total number of counts in both the β-decay channel (N_T^{β}) and βn-decay channel ($N_T^{\beta n}$) of assigned isotope, BR_{β} is the β-decay channel branching ratio.
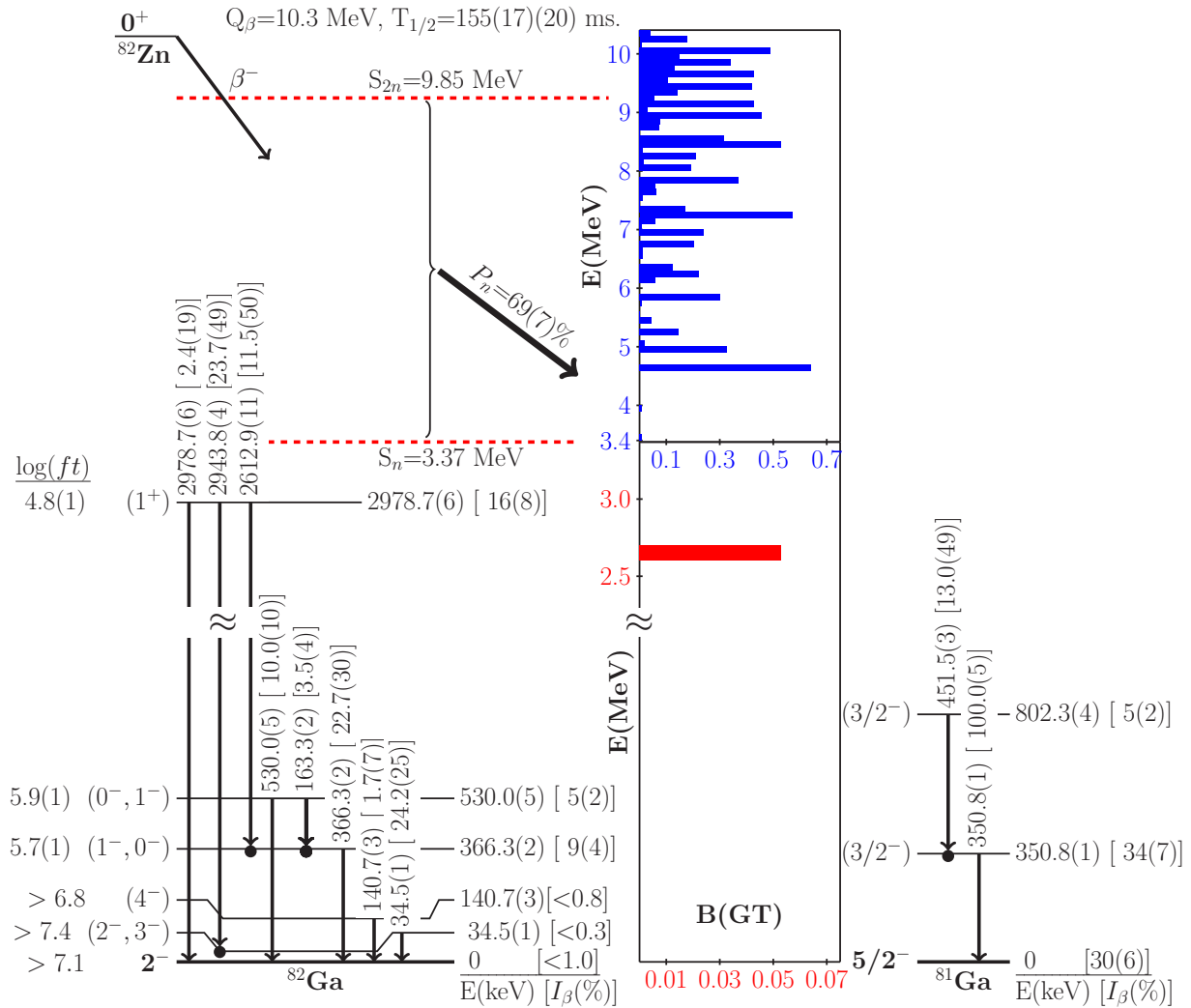
FIG. 7. Decay scheme of ^{82}Zn including all the observed γ-ray transition energies in keV followed by the intensities relative to strongest observed transition given in square brackets along with a theoretically calculated B(GT) matrix values vs the excitation energy in this decay. The experimentally calculated B(GT) for the 2978 keV level (0.06) is consistent with the theoretically predicted one. Note the scale change above and below S_n. The neutron's separation energies and neutron emission probability were taken from Ref. [25].

We conclude that the beam contained less than 10% of ^{82}Zn, and the rest (90%) was ^{82}Ga.

B. β decay of ^{83}Zn and ^{83}Ga

The β-gated γ-ray spectrum of the ^{83}Zn β-decay experiment is shown in Fig. 8. It is clearly seen that despite the suppression of ^{83}Ga activity through high-resolution mass separation, its β decay is dominant in this spectrum. The complexity of the ^{83}Ga precluded us from being able to determine the β-delayed neutron emission probability using the analysis of γ-ray intensities in the decay chain. However, a few new γ-ray transitions were identified in this experiment and the information on the low-energy levels in ^{83}Ga populated by the decay of ^{83}Zn is presented.

The γ spectrum in Fig. 8 represents the β- and βn-decay chain beginning from ^{83}Zn and ^{83}Ga, and ending with ^{83,82}As as shown in Fig. 9. The γ-γ coincidence spectra and/or the

half-life calculation were used to identify the β-decay parents for each single γ-ray transition in this spectrum.

1. Decay of ^{83}Zn

There is very little information available about ^{83}Zn except for the half-life and the observation of the 109 keV γ-ray transition [11]. From the analysis of γ-γ coincidence spectra shown in the top of Fig. 10, we concluded that the 109 keV line is a doublet γ-ray transition. Unfortunately, we cannot determine the exact energy values or intensities for each transition because the γ-ray detection resolution in this analysis is about 2 keV FWHM. We assign this doublet to be a cascade in ^{83}Ga based on the fact that neither of these transitions was previously reported in ^{82}Zn decay spectra. We did not observe a crossover transition with 218 keV, nor did we see any other γ-ray transition feeding ^{82}Ga energy states except the 141 keV isomeric γ-ray transition, which was fed into the β-delayed neutron emission branch. Because the

FIG. 8. Transitions from the decay of ^{83}Zn. The red numbers indicate ^{83}Zn β and βn decay, while the blue numbers indicate new γ-ray transitions in ^{83}Ga β decay. The ▼ represents known γ-ray transition in ^{83}As, the ♣ and ♠ represents γ-ray transitions in ^{82}Ge and ^{82}As, respectively. The ♦ symbol represents annihilation and neutron activation transitions and the ✳ symbol represents unassigned γ rays.

109 keV transition is prompt with β decay, both transitions are probably of M1 type. Figure 10 shows a simple ^{83}Zn β-decay scheme. On the other hand, we were able to see new γ-ray transitions in the ^{83}Ga β decay. Table II presents the relative intensities (I_γ) and their placement in a decay scheme enabled by the γ-γ coincidences of ^{83}Zn and ^{83}Ga γ-ray transitions.

An intriguing observation was made during the analysis of the ^{83}Ga decay. A 197.3 keV isomeric (120 ± 5 ns lifetime) transition was identified in the β-delayed γ-ray spectrum. The half-life of this transition measured with respect to the tape cycle was consistent with the ^{83}Ga-decay half-life. The presence of this transition can be explained as due to a neutron activation process. The inelastic scattering of high-energy neutrons [^{19}F($n,n'\gamma$)] [28] occurs on fluorine nuclei present in polytetrafluoroethylene (Teflon) material used to wrap the scintillator detectors in our experiment.

2. Decay scheme of ^{83}Ga

The analysis of γ rays that could be attributed to ^{83}Ga based on γ-γ coincidences (left-hand side of Fig. 11 and decay half-life analysis resulted in adding six new transitions and four new energy levels to the prior decay scheme of ^{83}Ga, as established by Winger *et al.* [10]. The updated ^{83}Ga β-decay scheme is shown in the right-hand side of Fig. 11. It is very clear that the 248 keV energy transition is a doublet with one transition from ^{82}Ge β decay and coincident with 843 keV and the other one from ^{83}Ga β decay. The intensity of

the 248 keV γ-ray transition in ^{83}Ga β decay is 4.4% of the 1092 keV intensity and is obtained by and accounting for the 3.4% absolute intensity from ^{82}Ge β decay [29].

We were unable to improve the data on neutron emission probability of ^{83}Ga βn decay. The previously measured value was reported to be $P_n = 62.8(25)\%$ [30]. Even though ^{82}Ge β decay has absolute intensities recently reported [29], the β-decay half-life of ^{82}Ge is twice as long as the MTC cycle decay time and only a small part of this isotope will decay before a new cycle begins. Because of these reasons, we were unable to extract new information on ^{83}Ga β-decay neutron emission probability [10] from these data.

FIG. 9. Decay chains observed in the ^{83}Zn decay experiment.

FIG. 10. Top shows the γ-γ coincidences of 109 keV in ^{83}Zn β decay. Bottom shows a simple decay scheme of ^{83}Zn. The neutron's separation energies were taken from Ref. [25].

TABLE II. Energy levels (E_{levels}) in ^{83,82}Ga and ^{83}Ge from β decay of ^{83,82}Zn and ^{83}Ga, respectively.

E_{level} (keV)	E_γ	I_γ	Final level (keV)
^{83}Zn β decay			
109	109		0
218	109		109
^{83}Zn βn decay			
141(1)	141(1)[a]		0
^{83}Ga β decay			
248.2(1)	248.2(1)	29(3)	0
1045.6(8)	797.9(3)[b]	4(1)	248.2(1)
	1045.6(8)	44(5)	0
1238.1(1)	1238.1(1)	100(8)	0
1245.7(1)	1245.7(1)[b]	17(2)	0
1452.0(4)	1204.1(2)[b]	14(2)	248.2(1)
	1452.0(4)[b]	13(3)	0
1941.2(2)	703.1(1)[b]	32(3)	1238.1(1)
2910.1(4)	2910.1(4)[b]	9(1)	0

[a]Isomeric γ transition.
[b]Observed for the first time.

The previous information was used to build the β-decay scheme of ^{83}Ga as presented in Fig. 11. The direct ground-state feeding between ^{83}Ga and ^{83}Ge was taken to be $\leqslant 34\%$ with $Q_\beta = 11.719(4)$ MeV [21], which is consistent with the previously reported one by Winger *et al.* [10]. The γ rays from the βn-decay channel are not added to this scheme. We observed γ-ray transitions at 415, 727, 867, 938, 985, 1176, 1348, 1354, 1365, and 2215 keV, which were previously reported by Winger *et al.* [10]. No new transitions were identified here.

C. ^{82,83}Zn half-lives

The grow-in and decay and decay-only patterns extracted from the energy vs MTC cycle time spectrum were used to calculate the half-lives. The background was subtracted by placing a gate in the region close to the γ-ray transition. The left and right background gate was used in this analysis, where it was selected symmetrically in the energy spectrum, with an equal number of channels left and right of the γ-ray transition. The background gate had in total the same number of channels as the γ transition gate. The resulting data were fitted with a nonlinear least-squares algorithm to Eq. (1). The first part of that equation represents the grow-in part of the cycle starting from zero to t_1. A is the implantation rate multiplied by the branching ratio of the gated γ-ray transition, which is a constant during the cycle time and treated as a fitting parameter. The second part is the natural decay part extended over the beam-off cycle from $t = t_1$ to $t = t_2$.

The half-life fitting analysis was tested using transitions from ^{82,83}Ga γ-ray spectra, which have known half-lives. In each test, we used both grow-in and decay and decay-only patterns; no significant difference was found between the two fits, and the final result was consistent with the reported values (see Fig. 12). The same method was used with ^{82,83}Zn, the average half-lives of these fits over the variation in subtracted

background using both grow-in and decay and decay-only gave 155(17) ms for ^{82}Zn and 122(28) ms for ^{83}Zn. The grow-in and decay fitting pattern of two selected β-gated γ-ray transitions are shown in Fig. 13.

Because the half-life value for ^{82}Zn is different by more than 3σ from the values reported by Madurga *et al.* [11], while it is consistent with one found by Xu *et al.* [12], we investigated the possible reasons for these inconsistencies in our data. It was found that the half-life calculation is sensitive to background subtraction procedure particularly for ^{82}Zn. As shown in Fig. 14, depending on the choice of background gate, the nonlinear least-squares fit can produce three different half-life values with very similar small χ^2. For this reason, we have to add a resulting uncertainty of 20 ms as a systematic error to the ^{82}Zn β-decay half-life to become 155(17)(20) ms. In the result, the ^{82}Zn half-life presented in Ref. [11] using the right gate only for background subtraction is therefore heavily affected by the time dependence observed here and it should be considered incorrect. The new shorter value presented here only strengthens the case made in [11] that global models systematically overestimates half-lives for nuclei close to shell closures.

IV. GAMOW-TELLER DECAYS OF ZINC AND GALLIUM ISOTOPES

β decays of $N > 50$ isotopes are a result of competition between forbidden transitions with large Q_β values but very small decay strength and allowed GT decays to highly excited states. The GT decay strength is large but can be very fragmented and difficult to observe in experimental data. For sufficiently exotic nuclei, the GT decay becomes dominant, resulting in the observation of large β-delayed neutron branching ratios [30,32–35] in this region [33,35]. The experimental results presented here show evidence for the GT transitions to the bound states in the decay daughter, thus providing insight into the role of the $N = 50$ shell gap in these decays. To quantify this observation, we have developed new shell-model calculations. To make such calculations feasible, we noted that the allowed GT transitions occur only between fpg neutrons and their spin-orbit partner proton orbitals inside the Q_β window, the neutrons occupying valence $d_{5/2}, s_{1/2}$ orbitals can be considered as spectators. Using this approximation, detailed shell-model calculations can be performed with the explicit inclusion of the $d_{5/2}$ orbital and with the relative spacing between $\nu d_{5/2}$ and the $\nu g_{9/2}$ ($N = 50$ shell gap) as a parameter of the model. In this case, the shell-model calculation used the interactions developed by Brown for the ^{78}Ni region, used previously to interpret experimental data near $Z = 28$ by Cheal *et al.* [36]. In the B(GT) calculation, the neutron $d_{5/2}$ orbital was added and a set of proton-neutron interactions was added, which were constructed schematically using the matrix elements for the $f_{5/2}$ orbital.

The calculation used the single particle energies -8.39 MeV ($f_{5/2}$), -8.54 MeV ($p_{3/2}$), -7.21 MeV ($p_{1/2}$), -5.86 MeV ($g_{9/2}$), and -1.98 MeV ($d_{5/2}$) for neutrons, and -14.94 MeV ($f_{5/2}$), -13.44 MeV ($p_{3/2}$), -12.04 MeV ($p_{1/2}$), and -8.91 MeV ($g_{9/2}$) for protons as proposed by Grawe *et al.* [37]. The shell-model code NUSHELLX was used in its parallel
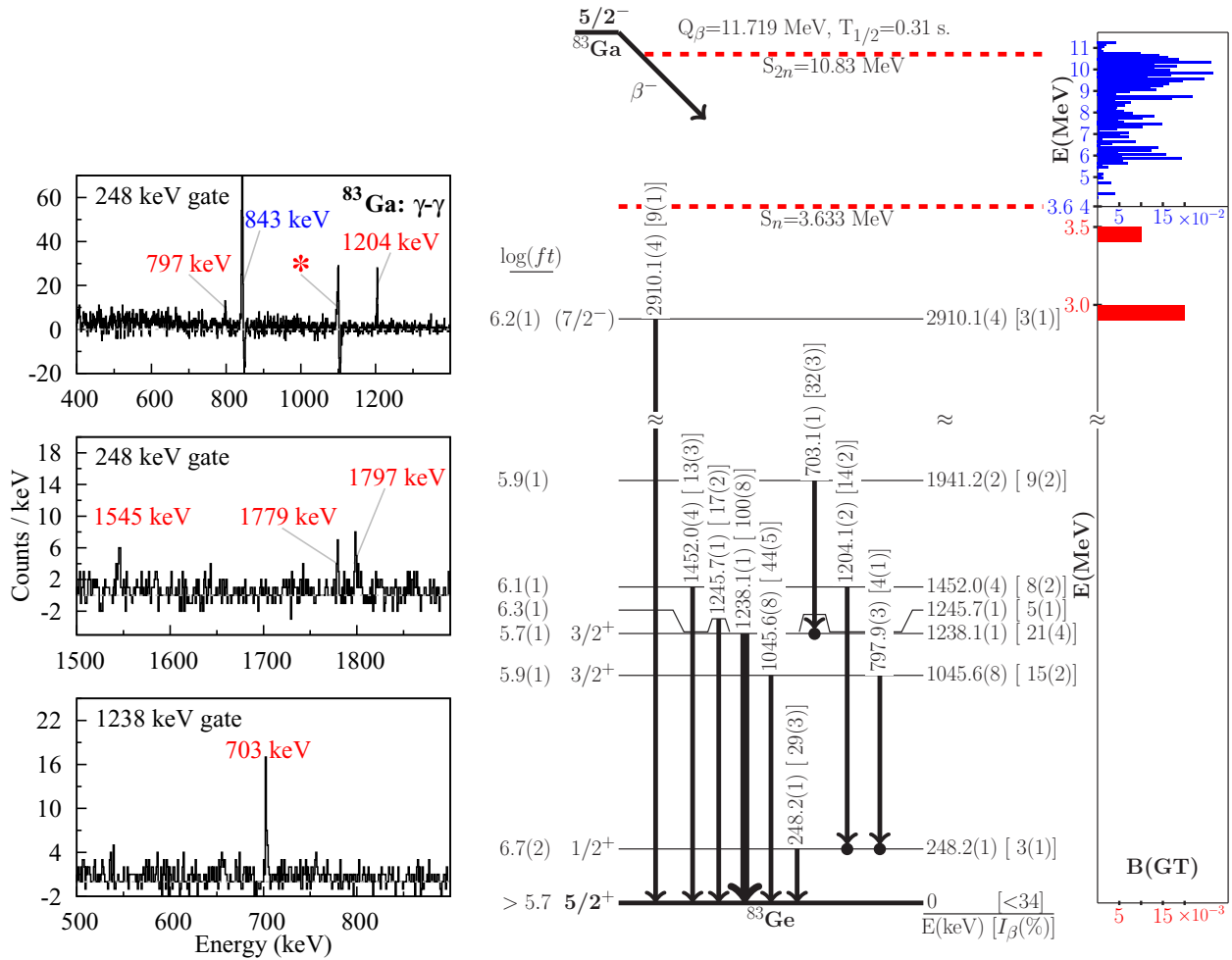
FIG. 11. Data analysis of ^{83}Ga β decay, where the left-hand side shows selected background subtracted γ-γ coincidences of related γ-ray transitions. The 843 keV line represents a γ-ray transition in ^{82}As and the ✲ symbol shows the Compton edge of 1348 keV γ-ray transition. The right-hand side shows the decay scheme of ^{83}Ga including all the observed γ-ray transition energies in keV followed by the intensities relative to strongest observed transition given in square brackets along with a theoretically calculated B(GT) vs the excitation energy in this decay. Note the scale change above and below S_n. The neutron's separation energies were taken from Ref. [25].

processing version [38,39] and calculations were performed on a 24-core machine. In these calculations, the neutrons occupying $d_{5/2}$ orbitals were blocked, while the protons and neutrons in their respective fpg orbitals were allowed to scatter without restrictions. The results of these calculations are presented in the right-hand panels in Figs. 4, 7, 10, and 11 for easy comparison with the experimental data. One easily notes that the majority of the GT strength distribution remains concentrated at high excitation energies of 5–6 MeV or more. In all of the investigated cases, this corresponds to population of neutron-unbound states, and explains the large β-delayed neutron branching ratios. In a few selected cases, the decay strength is scattered to lower energies, possibly due to proton-neutron interactions, and neutron bound states are populated. This is most dramatically seen in the ^{82}Zn decay, where a GT state at 2.6 MeV is predicted to exist. Experimental data revealed that a state at 2979 keV in ^{82}Ga is strongly populated in this decay. Based on the small $\log(ft) = 4.8$ value, we assigned this level to be 1^+. In the decay of ^{83}Zn, we could not assign unambiguously any of the transitions to be populating

any bound GT state. This is possibly due to the limited statistics and order of magnitude smaller B(GT) matrix elements for the states at about 4 MeV excitation than those for ^{82}Zn (see Fig. 10). Similarly, we can find a correspondence between the group of states above 5.6 MeV in ^{82}Ge and the low-energy fragments of the GT distribution (see Fig. 4). It is possible that the 4.221 MeV level is the lowest excited state populated via a GT transition. The very extended decay schemes observed in βn decays of ^{82}Ga and ^{83}Ga and population of states up to 3.5 MeV excitation energy in ^{81,82}Ge is also consistent with the concentration of β-decay strength predicted theoretically.

Closer inspection of the wave functions for all of the observed decays reveals that the majority of the strength involves the states with large amplitudes of $(\nu p_{1/2})^{-1}(\pi p_{3/2})$ or $(\nu p_{3/2})^{-1}(\pi p_{1/2})$ particle-hole excitation of the ^{78}Ni core coupled to neutrons in the $d_{5/2}$ orbital. However, the states we observed here, with relatively small B(GT)s, have configurations dominated by $d_{5/2}$ neutrons coupled to the $(\nu p_{3/2})^{-1}(\pi f_{5/2})$ excitation of ^{78}Ni. These, however, are not excitations that involve spin-orbit partners and hence are not connected with
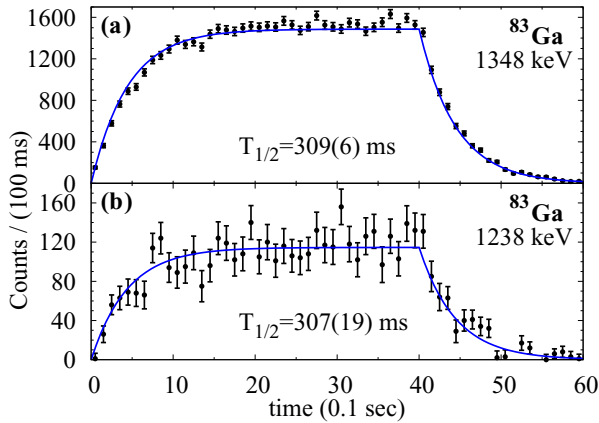
FIG. 12. Grow-in and decay fitting pattern for β-gated γ-ray transitions: (a) 1348 keV from ^{83}Ga βn decay and (b) 1238 keV from ^{83}Ga β decay. The blue lines represent the results of the least square fits. The two figures show β-decay half-lives of 309(6) and 307(19) ms, respectively, which is consistent with the previously reported one [31].

the GT operator. The strong pn interaction between $d_{5/2}$ neutrons and $f_{5/2}$ protons causes those states to be much lower in excitation energy and hence they provide the β-decay path to the bound states.

The unusually small B(GT) strength is due to configuration mixing. The small admixtures of the neutrons in $p_{1/2}$ and $p_{3/2}$ orbitals opens up the decay channels for the GT operator leading to small but observable strength. The phase space factor f will amplify the importance of the decays to the bound states with respect to higher-energy states. This feature may very strongly affect decay properties of nuclei closer to stability.

Only inclusion of the orbitals below the $N = 50$ shell closure can produce states in a daughter nucleus at sufficiently low energies, with spins and parities, which satisfy the GT selection rules. For example, focusing on the ^{82}Zn decay, in calculations with an inert ^{78}Ni core (as in Sec. V), the lowest 1^+ state in ^{82}Ga is predicted at 5.2 MeV and with a rather complex
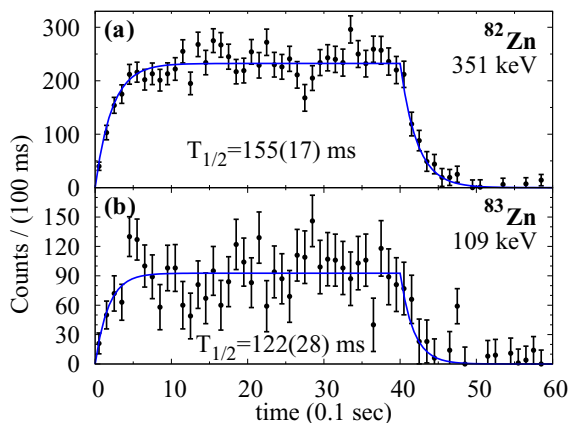
FIG. 13. Grow-in and decay fitting pattern for β-gated γ-ray transitions: (a) 351 keV from ^{82}Zn βn decay and (b) 109 keV from ^{83}Zn β decay. The blue lines show the results of the least square fits.
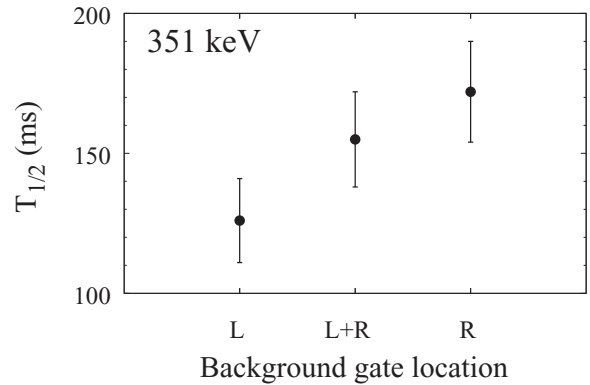
FIG. 14. The β-decay half-life of ^{82}Zn using the 351 keV γ-ray transition was found to depend on the background gate location, i.e., whether it is to the left (L) or the right (R) or split into two halves one to the left and one to the right (L+R).

wave function, and should be compared with the 2.6 MeV state predicted by the calculations with the ^{56}Ni core, and with the 2.98 MeV energy of the GT state found in experiment.

The explicit inclusion of the $d_{5/2}$ orbital in the calculations allowed us to investigate the dependence of the strength distribution of the shell-gap energy and we found a simple linear scalability of the distribution. The scalability is a result of the truncation of the model. The results of the calculations for the decay of ^{82}Ga are very consistent with the initial shell-gap energy of 3.88 MeV, which is compatible with the experimental results from mass measurement by Hakala *et al.* [40]. The ^{83}Zn decay data could point to a somewhat higher gap energy of about 4.2 MeV, but both results could be strongly affected by the choice of the pn interactions between particles in active orbitals and should be a subject for further theoretical work.

V. LOW-ENERGY EXCITED STATES IN GALLIUM AND GERMANIUM ISOTOPES

The low-energy excited states in gallium and germanium decays are populated in β decays either directly or via the deexcitation of the high-energy levels. Direct population occurs in forbidden type transitions, because parent ground state and daughter states are of opposite parity. This has been observed in all previous studies [10,22] and is evidenced by the large $\log(ft)$ values of about 5.5–6.5. While the states populated in GT decays are due to particle-hole excitations across the $N = 50$ shell gap, the low-energy excitations can be interpreted as excitations involving orbitals near the Fermi energy. The experimental data can be compared to the predictions by the nuclear shell model, which gives insight into the microscopic nature of the low-energy states observed. The calculations were performed using NUSHELLX [38,39] code. In this case the tails of the B(GT), which might be contained within the decay energy (Q_β) may compete with forbidden transitions and generate threshold effects strongly affecting nuclear lifetimes.

For the nuclei with $N > 50$ we used the valence space with ^{78}Ni inert core and single-particle orbital $d_{5/2}$ (−11.3

FIG. 15. Shell-model calculations for the low-energy excited states of the indicated ^{82,83}Ga and ^{83}Ge isotopes, where the a_78kn4 interactions with ^{78}Ni core were used. For ^{82}Ge, the calculations used the ^{56}Ni core and jj44bpn interactions. Note the ^{82}Ga energy levels scale is different from the other isotopes energy levels scales.

MeV), $g_{7/2}$ (-7.6 MeV), $2d_{3/2}$ (-10.2 MeV), $s_{1/2}$ (-10.5 MeV), and $h_{11/2}$ (-6.3 MeV) for neutrons and $f_{5/2}$ (-25.3 MeV), $p_{3/2}$ (-24.8 MeV), $p_{1/2}$ (23.6 MeV), and $g_{9/2}$ (20.3 MeV) for protons. The residual interactions "a_78kn4" [41] were derived [42] from chiral N3LO [43] nucleon-nucleon interactions. The results of these calculations for excited states in ^{82,83}Ga and ^{83}Ge are shown in Fig. 15. The low-energy excitation states in gallium isotopes are of negative parity and are dominated by the $d_{5/2}$ and $s_{1/2}$ neutrons coupled to $f_{5/2}$ protons forming a dense spectrum of levels.

The ^{82}Ga ground state, which is known to be $J^\pi = 2^-$ state [19] from laser spectroscopy, is calculated to be 172 keV above the predicted $J^\pi = 0^-$ ground state. This result is well within the accuracy expected by any shell-model calculation, especially for odd-odd nuclei. The long-lived (4^-) state observed by Kameda and in this work is also predicted to be isomeric by the shell model. This state is likely due to an aligned proton-neutron configuration between a $f_{5/2}$ proton and a $d_{5/2}$ neutron. The intensity of the 141 keV transition depopulating the 4^- state is very small $I_\gamma < 1.8\%$ and this state is unlikely to be populated directly in the β decay of even-even ^{82}Zn. This state is also observed in βn decay of ^{83}Zn. The new cascade of two 109 keV M1 transitions in ^{83}Ga can be explained as a set of transitions between low-energy $5/2^-$, $3/2^-$, and $1/2^-$ states also predicted by the shell model. However, the experimental data suggest a different ordering of the levels such as $1/2^-$, $3/2^-$, $5/2^-$. The predicted shell-model sequence requires that the low-energy E2 $1/2^-$-$5/2^-$ transition would result in an isomeric $1/2^-$ state. For completeness we also include calculations for positive parity states in ^{83}Ge. The inspection of the wave functions of the $1/2^+$ and $5/2^+$ states reveals a similar degree of configuration mixing as previously

published [44]. In these calculations, the first excited $1/2^+$ state in ^{78}Ni is at 0.768 MeV. For $N = 50$ ^{82}Ge, the calculations with a ^{78}Ni core are not appropriate, because of the missing proton-neutron correlations. For completeness, we show here the comparison with the calculations using the ^{56}Ni core and fpg proton and neutron valence space with interactions developed by Cheal [36]. These calculations reproduce very well the excitation energy of the 2^+ excited state.

VI. SUMMARY

In this work, we have measured and analyzed β decays of neutron-rich ^{82,83}Zn and ^{82,83}Ga isotopes. The experiments were performed using radioactive ion beams that were produced using the ISOL technique at the Holifield Radioactive Ion Beam Facility in ORNL.

The grow-in and decay patterns were fitted using a nonlinear least-squares algorithm to calculate the half-lives of ^{82,83}Zn and ^{82,83}Ga. The half-lives of ^{82,83}Ga were found to be in perfect agreement with previously published values. New half-lives of 155(17)(20) and 122(28) ms were determined for ^{82,83}Zn, respectively. These half-lives are slightly different from previously published values [11,12]. The differences were attributed to the different background subtraction methods.

New γ-ray transitions and high-energy levels in ^{82}Zn β decay were found and used to build a new decay scheme, where a $69 \pm 7\%$ β-delayed neutron branching ratio was determined. One doublet of γ-ray transition was found in ^{83}Zn decay and assigned to β-γ decay to low-energy ^{83}Ga levels. New γ-ray transitions and high-energy levels in ^{82,83}Ga β decay were also established and added to the recently published decay schemes [9,10].

Theoretical shell-model calculations were performed using the NUSHELLX computer code and revealed GT transitions associated with high-energy levels in ^{82,83}Zn and ^{82,83}Ga. The observed B(GT) values confirm our assumption of the existence of particle-hole excitation in the daughter nuclei.

Our experimental finding should be confirmed and expanded in total γ absorption and neutron spectroscopy experiments. Such studies will provide more complete data on β-decay strength distributions, which can form a basis for a complete and consistent theoretical description.

APPENDIX

Several transitions with no observed γ-γ coincidences were newly observed, and for the following reasons we placed them in the β-decay channel.

In the case of ^{82}Ga decay, we have 1951, 2826, 3076, 3571, 3848 keV γ-ray transitions that have no observed γ-γ coincidences, and for the following reasons we placed them in a β channel. The 3076 keV line is a crossover γ-ray transition for the 1727.4 and 1348.3 keV and can be assigned to ^{82}Ge. The 1951, 2826, 3076, 3571, and 3848 keV transitions were not observed previously in ^{81}Ga β decay, which was extensively studied previously (see, e.g., Ref. [27]) while all the other lines observed in βn channels of ^{82}Ga are also observed in a very extensive ^{81}Ga decay scheme.

In the case of ^{83}Ga decay, there are 1245.7, 1452.0, and 2910.1 keV γ-rays. The case in favor of assigning them to the ^{83}Ge level scheme is based on the following arguments. Among the previously reported [10] transitions in the βn channel of ^{83}Ga (415, 727, 867, 938, 985, 1176, 1348, 1354, 1365, and 2215 keV) all but the 727 keV were also observed in ^{82}Ga presented here. The 1245.7, 1452.0, and 2910.1 keV γ rays are not present in the ^{82}Ga decay data. The 2910 keV line is observed with a similar level of statistics as 2713 keV line, which is assigned to ^{83}Ga β-delayed neutron channel and is also observed in ^{82}Ga decay. The 2910 keV line is not observed in ^{82}Ga decay. Also, the 2910 keV was not observed in the neutron gated data taken in the later experiment using neutron detectors [11]. Additionally, the ^{83}Ga βn-γ decay channel has to proceed via 1348 keV first excited state in ^{82}Ge. Therefore the transitions 1245 keV (< 1348 keV), would have to be observed in coincidence with 1348 keV, if it were associated with the βn channel.

[1] T. Yoshida and A. Nichols, Assessment of fission product decay data for decay heat calculations: A report by the working party on international evaluation co-operation of the nuclear energy agency nuclear science committee, NEA Report No. 6284, 2007 (unpublished).

[2] D. A. Dwyer and T. J. Langford, Phys. Rev. Lett. **114**, 012502 (2015).

[3] F. P. An, J. Z. Bai et al., Phys. Rev. Lett. **108**, 171803 (2012).

[4] J. C. Hardy and I. S. Towner, Phys. Rev. C **71**, 055501 (2005).

[5] R. Surman, M. Mumpower, J. Cass, I. Bentley, A. Aprahamian, and G. McLaughlin, in *EPJ Web of Conferences*, Vol. 66 (EDP Sciences, Les Ulis, 2014), p. 07024.

[6] K. L. Kratz et al., Astrophys. J. **403**, 216 (1993).

[7] K. Grotz and H. V. Klapdor, *The Weak Interaction in Nuclear, Particle and Astrophysics* (CRC Press, Boca Raton, 1990).

[8] E. J. Konopinski and G. E. Uhlenbeck, Phys. Rev. **60**, 308 (1941).

[9] J. K. Tuli, Nucl. Data Sheets **98**, 209 (2003).

[10] J. A. Winger, K. P. Rykaczewski, C. J. Gross, R. Grzywacz, J. C. Batchelder, C. Goodin, J. H. Hamilton, S. V. Ilyushkin, A. Korgul, W. Krolas, S. N. Liddick, C. Mazzocchi, S. Padgett, A. Piechaczek, M. M. Rajabali, D. Shapira, E. F. Zganjar, and J. Dobaczewski, Phys. Rev. C **81**, 044303 (2010).

[11] M. Madurga, R. Surman, I. N. Borzov, R. Grzywacz, K. P. Rykaczewski, C. J. Gross, D. Miller, D. W. Stracener, J. C. Batchelder, N. T. Brewer, L. Cartegni, J. H. Hamilton, J. K. Hwang, S. H. Liu, S. V. Ilyushkin, C. Jost, M. Karny, A. Korgul, W. Krolas, A. Kuzniak, C. Mazzocchi, A. J. Mendez, K. Miernik, S. W. Padgett, S. V. Paulauskas, A. V. Ramayya, J. A. Winger, Wolinska-M. Cichocka, and E. F. Zganjar, Phys. Rev. Lett. **109**, 112501 (2012).

[12] Z. Y. Xu, S. Nishimura, G. Lorusso, F. Browne, P. Doornenbal, G. Gey, H. S. Jung, Z. Li, M. Niikura, P. A. Soderstrom, T. Sumikama, J. Taprogge, Z. Vajta, H. Watanabe, J. Wu, A. Yagi, K. Yoshinaga, H. Baba, S. Franchoo, T. Isobe, P. R. John, I. Kojouharov, S. Kubono, N. Kurz, I. Matea, K. Matsui, D. Mengoni, P. Morfouace, D. R. Napoli, F. Naqvi, H. Nishibata, A. Odahara, E. Sahin, H. Sakurai, H. Schaffner, I. G. Stefan,

D. Suzuki, R. Taniuchi, and V. Werner, Phys. Rev. Lett. **113**, 032505 (2014).

[13] J. R. Beene et al., J. Phys. G **38**, 024002 (2011).

[14] D. Stracener, HRIBF RIB Intensities, http://www.phy.ornl.gov/hribf/beams/rib-intensity-2007.shtml, 2007.

[15] http://www.xia.com/DGF_Pixie-16.html, 2008.

[16] D. Kameda et al., Phys. Rev. C **86**, 054319 (2012).

[17] P. Hoff and B. Fogelberg, Nucl. Phys. A **368**, 210 (1981).

[18] R. A. Warner and P. L. Reeder, Radiat. Eff. **94**, 27 (1986).

[19] B. Cheal et al., J. Phys.: Conf. Ser. **381**, 012071 (2012).

[20] B. Singh et al., Nucl. Data Sheets **84**, 487 (1998).

[21] M. Wang et al., Chinese Phys. C **36**, 1603 (2012).

[22] S. Padgett, M. Madurga, R. Grzywacz, I. G. Darby, S. N. Liddick, S. V. Paulauskas, L. Cartegni, C. R. Bingham, C. J. Gross, K. Rykaczewski, D. Shapira, D. W. Stracener, A. J. Mendez, J. A. Winger, S. V. Ilyushkin, A. Korgul, W. Krolas, E. Zganjar, C. Mazzocchi, S. Liu, J. H. Hamilton, J. C. Batchelder, and M. M. Rajabali, Phys. Rev. C **82**, 064314 (2010).

[23] J. A. Winger, J. C. Hill, F. K. Wohn, R. L. Gill, X. Ji, and B. H. Wildenthal, Phys. Rev. C **38**, 285 (1988).

[24] P. Hoff, K. Aleklett, E. Lund, and G. Rudstam, Z. Phys. A **300**, 289 (1981).

[25] National Nuclear Data Center (NNDC) in Brookhaven National Laboratory, Chart of Nuclides, http://www.nndc.bnl.gov/chart/.

[26] J. K. Hwang, J. H. Hamilton, A. V. Ramayya, N. T. Brewer, Y. X. Luo, J. O. Rasmussen, and S. J. Zhu, Phys. Rev. C **84**, 024305 (2011).

[27] C. M. Baglin, Nucl. Data Sheets **109**, 2257 (2008).

[28] R. B. Day, Phys. Rev. **102**, 767 (1956).

[29] K. Miernik, K. P. Rykaczewski, C. J. Gross, R. Grzywacz, M. Madurga, D. Miller, J. C. Batchelder, N. T. Brewer, C. U. Jost, K. Kolos, A. Korgul, C. Mazzocchi, A. J. Mendez, Y. Liu, S. V. Paulauskas, D. W. Stracener, J. A. Winger, Wolinska-M. Cichocka, and E. F. Zganjar, Phys. Rev. C **90**, 034311 (2014).

[30] J. A. Winger, S. V. Ilyushkin, K. P. Rykaczewski, C. J. Gross, J. C. Batchelder, C. Goodin, R. Grzywacz, J. H. Hamilton, A. Korgul, W. Krolas, S. N. Liddick, C. Mazzocchi, S. Padgett, A.

Piechaczek, M. M. Rajabali, D. Shapira, E. F. Zganjar, and I. N. Borzov, Phys. Rev. Lett. **102**, 142502 (2009).

[31] S.-C. WU, Nucl. Data Sheets **92**, 893 (2001).

[32] I. N. Borzov, Phys. Rev. C **71**, 065801 (2005).

[33] I. N. Borzov, Phys. Rev. C **67**, 025802 (2003).

[34] T. Rauscher, R. Bieber, H. Oberhummer, K. L. Kratz, J. Dobaczewski, P. Moller, and M. M. Sharma, Phys. Rev. C **57**, 2031 (1998).

[35] P. Moller, B. Pfeiffer, and K. L. Kratz, Phys. Rev. C **67**, 055802 (2003).

[36] B. Cheal, E. Mane, J. Billowes, M. L. Bissell, K. Blaum, B. A. Brown, F. C. Charlwood, K. T. Flanagan, D. H. Forest, C. Geppert, M. Honma, A. Jokinen, M. Kowalska, A. Krieger, J. Kramer, I. D. Moore, R. Neugart, G. Neyens, W. Nortershauser, M. Schug, H. H. Stroke, P. Vingerhoets, D. T. Yordanov, and M. Zakova, Phys. Rev. Lett. **104**, 252502 (2010).

[37] H. Grawe, in *The Euroschool Lectures on Physics with Exotic Beams, Vol. I*, edited by J. Al-Khalili and E. Roeckl (Springer, Berlin, Heidelberg, 2004), pp. 33–75.

[38] W. Rae, NUSHELLX, http://www.garsington.eclipse.co.uk, 2008.

[39] B. Brown and W. Rae, Nucl. Data Sheets **120**, 115 (2014).

[40] J. Hakala, S. Rahaman *et al.*, Phys. Rev. Lett. **101**, 052502 (2008).

[41] A. Signoracci (private communication).

[42] M. Hjorth-Jensen *et al.*, Phys. Rep. **261**, 125 (1995).

[43] D. R. Entem and R. Machleidt, Phys. Rev. C **68**, 041001 (2003).

[44] J. S. Thomas, D. W. Bardayan, J. C. Blackmon, J. A. Cizewski, U. Greife, C. J. Gross, M. S. Johnson, K. L. Jones, R. L. Kozub, J. F. Liang, R. J. Livesay, Z. Ma, B. H. Moazen, C. D. Nesaraja, D. Shapira, and M. S. Smith, Phys. Rev. C **71**, 021302 (2005).